Geologic Map of the Southern San Luis Basin, Taos County, New Mexico

by

Paul W. Bauer[1], Keith I. Kelson[2], Ren A. Thompson[3], and Mark M. Mansell[1]

[1]*New Mexico Bureau of Geology and Mineral Resources, 801 Leroy Place, Socorro, NM 87801*
[2]*William Lettis and Associates, Inc., 1777 Botelho Dr., Suite 262, Walnut Creek, CA, 94596*
[3]*U.S. Geological Survey, Box 25046, MS 980, Denver Federal Center, Denver, CO 80225*

October 2021

New Mexico Bureau of Geology and Mineral Resources
Open-file Digital Geologic Map OF-GM 294

Scale 1:24,000

Compilation of these six quadrangles was funded by a matching-funds grant from the STATEMAP program of the National Cooperative Geologic Mapping Act (Fund Number: G20AC00250), administered by the U. S. Geological Survey, and by the New Mexico Bureau of Geology and Mineral Resources, (Dr. Nelia W. Dunbar, *Director and State Geologist*; Dr. J. Michael Timmons, *Assoc. Director for Mapping Programs*).

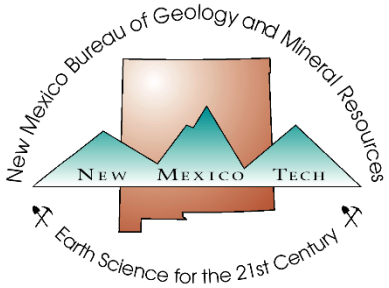

New Mexico Bureau of Geology and Mineral Resources
801 Leroy Place, Socorro, New Mexico, 87801-4796

Geologic Mapping and Cross Sections

The geologic maps used in this compilation combine six geologic maps of 7.5-minute quadrangles that were completed under the NMBGMR STATEMAP Program. The maps are credited as follows:

1) Taos 7.5-min quadrangle (Bauer and Kelson, 2001)
2) Los Cordovas 7.5-minute quadrangle (Kelson and Bauer, 2003)
3) Arroyo Hondo 7.5-minute quadrangle (Kelson and Bauer, 2006)
4) Guadalupe Mountain 7.5-minute quadrangle (Kelson, Thompson, and Bauer, 2008)
5) Arroyo Seco 7.5-minute quadrangle (Kelson, Bauer, and Rawling, 2010)
6) Questa 7.5-minute quadrangle (Kelson, Bauer, and Thompson, 2013)

Geologic mapping was done principally by Keith Kelson, Paul Bauer, and Ren Thompson between 1999 and 2013. Kelson focused on air photo interpretation, geologic and geomorphic mapping of surficial deposits and Tertiary rocks, and fault scarps in Quaternary deposits. Bauer focused on mapping the basement rocks and structures. Thompson focused on mapping the volcanic rocks.

The compilation map shows the distribution of rock units and unconsolidated, surficial, sand and gravel deposits, as well as the locations of known and inferred faults. Some of the geologic units shown in the cross sections are not exposed at the surface in the study area, but are exposed in nearby areas where they have been mapped and analyzed. The physical characteristics of some of these units (such as composition, thickness, texture, and lateral extent) are based on work in these nearby areas.

A primary goal was to provide a conceptual model of the large-scale geologic structure of the rift basins using geologic cross sections. Our approach was to understand the surficial structural geology around the edge of the basin by detailed mapping, and then to infer the subsurface basin structure using that knowledge and all other available data sets, including:

- photographic imagery
- boreholes
- geophysics
- surface structure
- geomorphology

- hydrology

The locations of the cross sections were chosen to optimize geologic and hydrogeologic understanding, maximize the number of useful wells that could be incorporated into the section lines, and utilize the geophysical insights provided by our U.S. Geological Survey colleagues Dr. V.J.S. Grauch and Dr. Benjamin J. Drenth. The topographic profiles were generated by ArcGIS software.

The geologic units shown in the cross sections originated from three principal data sources:

1) 1:24,000 geologic quadrangle maps
2) Interpretations from borehole geology and borehole geophysics
3) Interpretations from three geophysical data sets—a high-resolution aeromagnetic survey, ground-magnetic surveys, and gravity modeling

The relevance of the various data sets used to create the geologic map and cross sections is summarized below.

AERIAL PHOTOGRAMMETRY AND FIELD MAPPING

As part of delineating bedrock units, faults, and basin-fill sediments, the mappers analyzed multiple sets of photographic imagery, all of which have a high degree of clarity and provide good information on surficial deposits and fault-related features.

Because of their good coverage and high quality, the air-photo analysis primarily utilized 1:15,840-scale color images taken for the USFS from 1973–1975. Following our analysis of aerial photography, we conducted detailed mapping of geologic units and geomorphic features at scales of 1:24,000, 1:12,000, and 1:6,000. Our mapping delineated Quaternary deposits and surfaces, and Quaternary faults, fault scarps, and lineaments. Analysis of faults in all units (Proterozoic to Quaternary) included evaluations of fault geometries and kinematic data.

On bedrock faults, fault striations (slickenlines) were combined with kinematic indicators such as offset piercing lines or planes, and calcite steps to infer slip directions. Because of limited fault exposures in Quaternary deposits, we inferred slip directions based on fault scarp geometry, the map pattern of fault strands, and deflected drainages.

The fault structures depicted in the cross sections were established from three data sources:

1) Mapped faults from the geologic map
2) Inferred faults from USGS magnetic and gravity surveys
3) A conceptual model of the geometry and kinematics of the northern Rio Grande rift

Each of these three data sets is summarized below. Readers should note that imposing a vertical exaggeration on cross sections results in the apparent steepening of faults. Based on measurements of faults exposed in the Sangre de Cristo Mountains, the average dip of faults in this area is approximately 60 to 70 degrees. On the exaggerated cross sections, these dips appear steeper.

1) The geologic maps show a large number of segmented, normal fault splays along the Sangre de Cristo fault zone east of Questa, and other zones of faults within the rift basin. On the cross sections, such faults are labeled "mapped fault."
2) Modern geophysical techniques using high-resolution magnetic and gravity data (Grauch et al., 2015) are capable of defining buried faults in Rio Grande rift basins, such as in the Questa area. U.S. Geological Survey geophysicists Dr. V.J.S. Grauch and Dr. Benjamin J. Drenth have refined these techniques in the Rio Grande rift. They are currently capable of processing these data in ways that allow them to draw the locations of faults that generate geophysical anomalies. On the cross sections, such faults are labeled "geophysical fault." It is worth noting that there is good correlation between the mapped faults and the geophysically defined faults. Such correspondence elevates our confidence in the delineation of buried faults by such geophysical techniques. Recent gravity modeling by Dr. Drenth provides a useful tool for estimating the thickness of basin-fill deposits in the rift basin. This technique yields a depth-to-basement curve for the cross sections. As the basement deepens away from the edge of the rift, numerous buried faults must exist in order to deepen the basement. On the cross sections, such faults are labeled "inferred fault."
3) The conceptual geologic model for the development of this part of the southern San Luis basin of the Rio Grande rift (Kelson et al., 2008, 2013), provides a framework for presenting the geometry and kinematics of the local rift structures. In the Questa area, the west-down normal faults of the Sangre de Cristo fault system are expected to be the dominant buried features, although the Red River fault is an east-down, normal fault zone.

DEVELOPMENT OF CROSS SECTIONS

The following list describes the general steps that were taken to create the geologic cross sections developed for this map:

1) Geologic contacts were derived from the geologic map. The surface geology was taken from the geologic map and placed on the topographic profile of the cross sections. Geologic contacts that are buried by thin surficial deposits were estimated. Some of the thinnest (generally less than several meters) Quaternary surficial deposits are not shown on the cross sections.

2) The gravity model was used to define the depth-to-basement rocks in the cross sections. The bases of the cross sections are constrained by the depth-to-basement curve derived from the USGS gravity model. The depth-to-basement curve depicts a highly smoothed contact between basin-fill sediments and bedrock. In the model, Tertiary igneous rocks of the Questa caldera/Latir volcanic field and Proterozoic crystalline rocks are considered to be bedrock.

3) Geologic information derived from the wells was added to the cross sections. Poorly studied wells have limited value for developing cross-section stratigraphy, especially for the basin-fill sediments. However, expertly studied wells can help define the regional thicknesses and depths of key stratigraphic formations, including some of the basin-fill units such as the Lama Formation and thick clay horizons. Most of the basin-fill stratigraphy (including the Santa Fe Group, Chamita Formation, and Lama Formation) consists of poorly sorted, clay-to-boulder sized, alluvial material that was eroded from the nearby mountains. Unless the compositions and proportions of rock clasts and the color of the sediment are well described, it is not possible to tell them apart in drill holes. Although the depictions of these units on the cross sections are based principally on borehole data, local stratigraphic relationships, and an understanding of the sedimentary systems and geologic processes of the area, it is possible that the thicknesses of the various basin-fill units are not accurately represented. For example, it is generally not possible to confidently place the contact between the Chamita Formation and the Lama Formation where the Servilleta Formation is absent.

4) Mapped and inferred faults are drawn onto the cross sections. For the purposes of this study, the dips of the inferred faults were estimated to be between 60 and 70 degrees westward, unless evidence existed for some other orientation. In all cases, the geometries of the normal faults drawn in the cross sections are intentionally simplified as single inclined planes, when in fact all of the mapped normal faults in this area have much more complex geometries. They are typically curved, segmented, branched, and composed of multiple overlapping fault planes. Where exposed, faults in bedrock typically display wide fracture zones with high permeabilities, whereas faults in basin-fill sediments commonly display narrow, clay-rich cores with lower permeabilities.

5) Interpretations from geophysics are added to cross sections. Additional information gleaned from the geophysical work is added to the cross sections. For example, this includes evidence for buried volcanic rocks or for differentiating buried volcanic rocks into separate volcanic units (Grauch et al., 2015).

6) Conceptual models of volcanic and sedimentary processes are incorporated into cross sections. This phase of work was principally done by USGS geologist Dr. Ren Thompson, who used his extensive knowledge of the Taos Plateau volcanic field to draw realistic configurations of the buried volcanoes and their surroundings.

7) Information from the hydrology is added to the cross sections. Hydrologic information such as the locations of spring zones, streams and acequias, water levels in wells, and variations in field parameters, such as groundwater temperature, may be included on the cross sections. Based on past hydrogeologic studies of springs elsewhere in Taos County, we have found that the location and characteristics of springs are strongly influenced by the geology. Specifically, springs tend to occur where contrasts in hydraulic permeability exist. Such contrasts can be created by faulting, by primary variations in rock properties, and by post-depositional effects such as cementation.

8) Formation contacts are drawn onto the cross sections. Due to a lack of stratigraphic markers in the Questa/Taos area, the dips of the geologic units are unknown. Therefore, unless evidence exists for depicting local dips, contacts have been drawn as sub-horizontal. In most areas of the study area, thicknesses of buried basin-fill units are unknown. As a general rule, basin-fill units become thinner from west to east, following the deepest part of the basin to the bedrock of the Sangre de Cristo Mountains.

9) The cross section is checked against the geophysical models. After the cross sections were drawn, they were checked by our USGS colleagues against the geophysical models derived from the aeromagnetic and gravity surveys. If the geophysical model is robust, this is an excellent way to fine-tune the geologic model. For example, the aeromagnetic model might suggest that the thickness of a volcanic layer in a cross section needs to be adjusted, or that a fault must juxtapose materials with different magnetic properties. This iterative process between geologic and geophysical models was a powerful tool for developing a well-constrained geologic framework for the study area.

Description of Map Units

w **Water (Cenozoic)**—Surface water of the Rio Grande Corridor.

SEDIMENTARY ROCKS AND DEPOSITS OF THE RIO GRANDE RIFT AND ADJACENT HIGHLANDS

tailings **Tailings ponds (Cenozoic (modern-historic))**—Areas of artificially deposited fill and debris; delineated where aerially extensive; consists predominantly of mining-related mill tailings and tailings dams west of Questa; the geologic map shows the pre-tailings geology based on an interpretation of aerial photos.

af **Artificial fill and disturbed land (Cenozoic (modern-historic))**—Excavations and areas of human-deposited fill and debris; shown only where aerially extensive.

ds **Mine waste rock and related features (Cenozoic (modern-historic))**—Angular blocks and finer deposits, mainly from Tertiary plutonic rocks; principally located in and adjacent to the open pit molybdenum mine located in the Sangre de Cristo Mountains east of Questa.

Qal **Alluvium (latest Pleistocene and Holocene)**—Generally brownish and/or reddish, poorly to moderately sorted, angular to rounded, thinly to thickly bedded, loose silt and silty sand with subordinate coarse lenses and thin to medium beds of mostly locally derived clasts; mapped in active channels, floodplains, low (young) alluvial terraces, tributary-mouth fans, and some valley-slope colluvial deposits; weak to no soil development; clasts along the Rio Hondo are principally granitic rock types, quartzite, and basalt; clasts along tributaries draining the western side of the Rio Grande are principally volcanic rock types; clasts along the Rio Lucero are principally granitic rock types with some quartzite; clasts along the Rio Pueblo de Taos are principally granitic rock types, quartzite, and sandstones; drainages south and east of the Rio Pueblo de Taos are dominated by sandstone and other sedimentary rock types; clasts in the Taos and Los Cordovas quadrangles are principally granitic, metamorphic, volcanic, and sandstone rock types; up to 7 m estimated thickness.

Qm **Marsh deposits (Holocene)**—Silt, sand, and clay in low relief, saturated flatlands; high organic content; hosts a variety of streams, springs, and bogs; located primarily between US-64 and Taos Pueblo, bordering the Rio Lucero.

Qc **Colluvium (middle Pleistocene to Holocene)**—Mostly locally derived, light- to dark-brown, orange, and rarely reddish, poorly to moderately sorted, angular to well-rounded, silty to sandy conglomerate/breccia with clasts locally to >1m; mapped on hill slopes and valley margins only where it obscures underlying relations; mantles slopes in Red River gorge and northeastern side of Red River fault zone in the eastern part of the Guadalupe Mountain quadrangle; widespread along the bases of mountain-front facets; dominated by quartzite and granitic rock types north of the Rio Pueblo de Taos; dominated by sandstone and pebble conglomerate with minor limestone clasts south of the Rio Pueblo de Taos; in the northwestern part of the Arroyo Hondo quadrangle, west of the Rio Grande, the deposits consist of thin mantles overlying volcanic bedrock; estimated at generally less than 5 m thick.

Qs **Talus and scree (Pleistocene to Holocene)**—Angular rock fragments as much as 1 m in diameter forming talus cones, talus aprons, and scree slopes; locally well sorted; grades into colluvium as sand and silt content increases; shown only in the Sangre de Cristo Mountains by Lipman and Read (1989).

Qad **Alluvium in closed depressions (latest Pleistocene to Holocene)**—Light to dark-brown, very thin- to medium-bedded, loose, massive, shady to silty beds with thin, discontinuous layers of pebbles and rare cobbles (to ~15 cm) found on Toreva (rotational) blocks associated with landslide complexes; local thickness of at least several meters.

Qsw **Sheetwash alluvium (late Pleistocene to Holocene?)**—Alluvial aprons composed mostly of pebbly to silty sand that accumulated on gentle slopes, such as those on Servilleta Basalt (**Tsb**); some of the silt- to fine sand-size fraction in these deposits may be of eolian origin (Shroba and Thompson, 1998); deposits of unit **Qsw** exist along the shores of intermittent ponds or small lakes on the Servilleta Basalt (**Tsb**); low-lying areas of unit **Qsw** are susceptible to sheet flooding due to unconfined overland flow, and locally to stream flooding and gullying; recently disturbed surface of unit **Qsw** may be susceptible to minor wind erosion; estimated thickness is 1 to 5 m, but possibly as much as 10 m (Thompson et al., 2014).

Qty **Young stream terrace deposits (latest Pleistocene to Holocene)**—Poorly sorted deposits of silt, sand, pebbles, cobbles and boulders; deposits are typically clast-supported and poorly bedded; pebble and cobble clasts are typically imbricated; terrace deposits unconformably overlie the local bedrock; clasts are primarily sedimentary rocks, quartzite, slate, schist, metavolcanic, granitic rocks, and Tertiary granitic and volcanic rocks; uppermost sediments are typically silty sand probably

deposited from overbank flow; weak to moderate pedogenic development, including A, Bw, Bwk and Bk soil horizons and stage I to II calcium carbonate development; map unit **Qty** is typically on valley floors of large to medium drainages, whereas **Qfy** exists as young mountain-front fans and valley fills in small tributaries; includes units **Qf6** along the mountain front (Arroyo Seco quadrangle), **Qt6** (Los Cordovas quadrangle) and **Qt8** (Arroyo Hondo and Arroyo Seco quadrangles) of Kelson (1986); thickness up to 5 m.

Qfy **Young alluvial-fan deposits (latest Pleistocene to Holocene)**—Poorly sorted deposits of silt, sand, pebbles, cobbles and boulders; deposits are typically clast-supported and poorly bedded; pebble and cobble clasts are typically imbricated; terrace deposits unconformably overlie the local bedrock; clasts are primarily sedimentary rocks, quartzite, slate, schist, metavolcanic, granitic rocks, and Tertiary granitic and volcanic rocks; uppermost sediments are typically silty sand probably deposited from overbank flow; weak to moderate pedogenic development, including A, Bw, Bwk and Bk soil horizons and stage I to II calcium carbonate development; map unit **Qty** is typically on valley floors of large to medium drainages, whereas **Qfy** exists as young mountain-front fans and valley fills in small tributaries; includes units **Qf6** along the mountain front (Arroyo Seco quadrangle), **Qt6** (Los Cordovas quadrangle) and **Qt8** (Arroyo Hondo and Arroyo Seco quadrangles) of Kelson (1986); thickness up to 5 m.

Qfyv **Young alluvial-fan deposits from volcanic terrane (latest Pleistocene to Holocene)**—Poorly sorted silt, sand, pebbles, cobbles, and boulders; clasts primarily of volcanic rock types; associated soils have stage I calcium carbonate development; source areas are primarily the volcanic terrane on west side of the Rio Grande and drainages on Guadalupe Mountain.

Qe **Eolian deposits (late Pleistocene to Holocene)**—Light-colored, well-sorted, fine to medium sand and silt deposits that are recognized as laterally extensive, low-relief, sparsely vegetated, mostly inactive, sand dunes and sand sheets that overlie Servilleta Basalt on the Taos Plateau; rare gravel lag; weak to moderate soil development; northeast-trending longitudinal dune-crest orientations indicate that the predominant wind direction was from the southwest; up to several meters thick.

Qls **Landslides in the Rio Grande gorge and tributaries (late Pleistocene to Holocene)**—Poorly sorted rock debris and sand to boulder debris transported downslope; occurs on slopes marked by hummocky topography and downslope-facing scarps; includes small earth flow, block-slump, and block-slide deposits; includes large rotational Toreva slide blocks within the Rio Grande and Rio Pueblo

de Taos gorges, which include large, rotated and detached blocks of intact Servilleta Basalt; may also include areas underlain by Holocene colluvium in the Rio Grande and Red River gorges.

Qlsm **Landslides in the Sangre de Cristo Mountains (Pleistocene to Holocene)**—Lobate accumulations of poorly sorted soil and rock debris on slopes marked by hummocky topography and downslope-facing scarps; derived from bedrock and glacial deposits, and includes small earth flow, block-slump, and block-slide deposits (from Lipman and Read, 1989).

Qfo **Alluvial fan deposits, undivided (middle to late Pleistocene)**—Poorly sorted silt, sand, pebbles, and cobbles; in the Guadalupe Mountain quadrangle, **Qfo** is composed primarily of intermediate and basaltic volcanic clasts; moderate pedogenic development, including A, Bt, Btk and Bk soil horizons and stage III and IV calcium carbonate development; upper soil horizons are commonly affected by surface erosion; probably overlaps with units **Qf2** through **Qf4**, and with alluvial units **Qt2** through **Qt6**, but not assigned to other fan units because of lack of well-defined age control, clear stratigraphic position, and distinct lithologic characteristics; thickness up to 3 m.

Qfu **Alluvial fan deposits, undivided (middle to late Pleistocene)**—Poorly sorted silt, sand, pebbles, and cobbles; mapped along majority of Sangre de Cristo range front, but not correlated to other fan units because of lack of well-defined age control, clear stratigraphic position, or distinct lithologic characteristics; probably correlative with alluvial fan deposits **Qf1** through **Qf6**.

Qmt **Moraine and till (Pleistocene)**—Terminal and lateral moraines, and thick valley-bottom till; poorly sorted and generally unstratified clay, silt, and sand containing erratic boulders; characterized by hummocky or ridged topography; some till is mapped with colluvium by Lipman and Read (1989), although some **Qmt** deposits were remapped in this study.

Qtu **Stream terrace deposits, undivided (middle to late Pleistocene)**—Poorly sorted silt, sand, pebbles, and boulders; clasts primarily of quartzite, schist, granite, and volcanic rock types; associated soils have stage II to III calcium carbonate development; typically present as thin (< 5 m) alluvial deposit on strath surfaces cut on volcanic bedrock or unit **QTl**; probably correlative with **Qt1** through **Qt4**.

Qf1 **Alluvial-fan deposits (middle Pleistocene)**—Poorly sorted silt, sand, pebbles, and boulders; stage III to IV calcium carbonate development, although soil horizons are

commonly affected by surface erosion; in the Los Cordovas quadrangle, the clasts are principally granitic, intermediate volcanic, basalt, and metamorphic rock types; granitic clasts are also present east of Arroyo del Alamo; in the Taos quadrangle, clasts are primarily granitic and metamorphic rock types; the deposit is finer grained to the north and away from the Picuris Mountains range front; **Qf1** is differentiated from **QTl** by larger clast size (Kelson, 1986), less oxidation, poor sorting, absence of abundant manganese oxide staining, and clasts that are less weathered; slope of **Qf1** surface on the Taos and Los Cordovas quadrangles is southwesterly, and is dissected by numerous southwesterly trending arroyos; on the Taos quadrangle, **Qf1** is correlative with unit **Q1p** of Kelson (1986); a tephra within **Qf1** deposits on the Taos SW quadrangle was dated at 1.27 ± 0.02 Ma (40Ar-39Ar method, W. McIntosh, personal comm., 1996); the deposit is more than 12 m thick in the northeastern part of Los Cordovas quadrangle, and is thinner from northeast to southwest; directly southwest of Taos Municipal Airport, **Qf1** is less than about 1 m thick and unconformably overlies Servilleta Basalt (**Tsb**); elsewhere, **Qf1** appears to overlie unit **QTl** or **Tsb**; **Qf1** is more than 12 m thick in the northwestern part of the Taos and Arroyo Hondo quadrangles, and is thinner from northeast to southwest; on Blueberry Hill, **Qf** is about 3 m thick at US-64, and about 2 m thick to the southwest, where it unconformably overlies the unit **QTl**; it is more than 5 m thick in the northeastern part of the Arroyo Seco quadrangle, and thins from northeast to southwest; it is more than 5 m thick in the northeastern part of the Questa quadrangle, and thins from northeast to southwest.

TERRACE DEPOSITS OF THE RIO GRANDE

Qao3 **Older alluvium (middle? Pleistocene)**—Poorly sorted silt, sand, and pebbles; clasts primarily of granitic, metamorphic, basaltic, and intermediate volcanic rocks; distinctly smaller clast sizes than units **Qt2rr**, **Qt1rr**, and **Qt0rr**; upper soil horizons are locally affected by surface erosion; may be mantled locally by unit **Qe**; typically present as thin (< 5 m) alluvial deposit on strath surfaces cut on volcanic bedrock near the rim of the Rio Grande gorge; located only upstream of the Red River fault zone; correlative with unit **Qao3** of Ruleman et al. (2007) in the Sunshine quadrangle.

Qt2rg **Stream terrace deposits of the Rio Grande (middle? Pleistocene)**—Poorly sorted silt, sand, pebbles, and boulders; clasts primarily of granitic, metamorphic, intermediate volcanic, basalt, and sedimentary rocks; locally contains clasts of Amalia Tuff; associated soils have stage III to IV calcium carbonate development, thick argillic Bt soil horizons, and 7.5YR to 10YR hues in soil Bt horizons; upper soil horizons may be affected by surface erosion; may be mantled locally by unit **Qe**;

possibly faulted by the Dunn fault in the Arroyo Hondo quadrangle; modified from Kelson (1986); estimated thickness 1 to 10 m.

Qt1rg **Stream terrace deposits of the Rio Grande (early to middle? Pleistocene)**—Poorly sorted sand, pebbles, and cobbles; clasts of basalt, quartzite, slate, schist, and other metamorphic rock types, volcanic rock types, and (rarely) sandstone and limestone; locally contains clasts of 25 Ma Amalia Tuff; where preserved, associated relict soils have stage III to IV calcium carbonate development, thick argillic Bt soil horizons, and 7.5YR hues in soil Bt horizons; upper soil horizons commonly affected by surface erosion; may be mantled locally by unit **Qe**; estimated thickness 1 to 10 m.

Qt0rg **Stream gravel deposited by the ancestral Rio Grande (early? to middle? Pleistocene)**—Poorly sorted sand, pebbles, and cobbles; clasts of basalt, quartzite, slate, schist, other metamorphic rock types, and volcanic rock types; very rare Amalia Tuff clasts; associated with the broad, highest terrace west of the Rio Grande; upper soil horizons commonly affected by surface erosion; locally mantled by eolian sand.

TERRACE DEPOSITS OF THE RIO PUEBLO DE TAOS

Qt7rp **Stream terrace deposits of the Rio Pueblo de Taos (early to middle Holocene)**—Poorly sorted silt, sand, pebbles, cobbles, and boulders; clasts primarily of quartzite, schist, granite, and volcanic rock types; associated soils have stage I calcium carbonate development; typically present as thin (< 5 m) alluvial deposit on strath surfaces cut on volcanic bedrock or unit **QTl**.

Qt6rp **Stream terrace deposits of the Rio Pueblo de Taos (latest Pleistocene)**—Poorly sorted silt, sand, pebbles, cobbles, and boulders; clasts primarily of quartzite, schist, granite, and volcanic rock types; associated soils have stage I to II calcium carbonate development; typically present as thin (< 5 m) alluvial deposit on strath surfaces cut on volcanic bedrock or unit **QTl**; associated with the **Q6** surface of Kelson (1986).—Poorly sorted silt, sand, pebbles, cobbles, and boulders; clasts primarily of quartzite, schist, granite, and volcanic rock types; associated soils have stage I to II calcium carbonate development; typically present as thin (< 5 m) alluvial deposit on strath surfaces cut on volcanic bedrock or unit **QTl**; associated with the **Q6** surface of Kelson (1986).

Qf4 **Alluvial-fan deposits of the Rio Pueblo de Taos and tributaries (middle? to late Pleistocene)**—Poorly sorted silt, sand, pebbles, and boulders; associated soils have

stage III calcium carbonate development, argillic Bt soil horizons and 10YR to 7.5YR hues in Bt horizons; clasts primarily of granitic and metamorphic rocks north of the Rio Pueblo de Taos, and granitic, metamorphic, and sedimentary rock types south of the Rio Pueblo de Taos; clasts also include basaltic rock types along Arroyo Seco and along the Rio Pueblo de Taos downstream of Los Cordovas; modified from Kelson (1986).

Qt4rp **Alluvial-fan and Stream terrace deposits of the Rio Pueblo de Taos and tributaries (middle? to late Pleistocene)**—Poorly sorted silt, sand, pebbles, and boulders; associated soils have stage III calcium carbonate development, argillic Bt soil horizons and 10YR to 7.5YR hues in Bt horizons; clasts primarily of granitic and metamorphic rocks north of the Rio Pueblo de Taos, and granitic, metamorphic, and sedimentary rock types south of the Rio Pueblo de Taos; clasts also include basaltic rock types along Arroyo Seco and along the Rio Pueblo de Taos downstream of Los Cordovas; modified from Kelson (1986).

Qt3rp **Alluvial-fan and stream terrace deposits of the Rio Pueblo de Taos and tributaries (middle? to late Pleistocene)**—Poorly sorted silt, sand, pebbles, and boulders; associated soils have stage II to III calcium carbonate development; clasts primarily of quartzite, slate, and schist; granitic clasts also exist east of Arroyo del Alamo; possible **Qt3rp** remnant inset into terrace **Qt2rp** on the western side of Taos may be an artificial terrace related to residential development; modified from Kelson (1986).

Qf2 **Alluvial-fan and stream terrace deposits of the Rio Pueblo de Taos and tributaries (middle? Pleistocene)**—Poorly sorted silt, sand, pebbles, and boulders; clasts primarily of granitic and metamorphic rocks north of Rio Pueblo de Taos, and granitic, metamorphic and sedimentary rocks south of Rio Pueblo de Taos; associated soils have stage III to IV calcium carbonate development, thick argillic Bt soil horizons, and 7.5YR to 10YR hues in soil Bt horizons; upper soil horizons may be affected by surface erosion; modified from Kelson (1986).

Qt2rp **Alluvial fan and stream terrace deposits of the Rio Pueblo de Taos and tributaries (middle? Pleistocene)**—Poorly sorted silt, sand, pebbles, and boulders; clasts primarily of granitic and metamorphic rocks north of Rio Pueblo de Taos, and granitic, metamorphic and sedimentary rocks south of Rio Pueblo de Taos; associated soils have stage III to IV calcium carbonate development, thick argillic Bt soil horizons, and 7.5YR to 10YR hues in soil Bt horizons; upper soil horizons may be affected by surface erosion; modified from Kelson (1986).

Qt1rp **Stream terrace deposits of the Rio Pueblo de Taos and tributaries (middle? Pleistocene)**— Poorly sorted silt, sand, pebbles, and boulders; clasts primarily of quartzite, slate, and schist; finer grained to the north, away from the Picuris Mountains range front; stage III to IV calcium carbonate development, although soil horizons are commonly affected by surface erosion; present along the west rim of the Rio Grande del Rancho valley; where exposed to the south of the mapped area, the unit is up to 12 m thick.

TERRACE DEPOSITS OF THE RIO HONDO

Qt8rh **Stream terrace deposits of the Rio Hondo (middle to late Holocene)**—Poorly sorted silt, sand, pebbles, cobbles, and boulders; clasts primarily of quartzite, schist, granite, and volcanic rock types; deposits have negligible soil development; typically present as thin (< 5 m) alluvial deposit beneath high-stage floodplain or adjacent to active alluvial channels.

Qt7rh **Stream terrace deposits of the Rio Hondo (early to middle Holocene)**—Poorly sorted silt, sand, pebbles, cobbles, and boulders; clasts primarily of quartzite, schist, granite, and volcanic rock types; associated soils have stage I calcium carbonate development; typically present as thin (< 5 m) alluvial deposit on strath surfaces cut on volcanic bedrock or unit **QTl**.

Qt6rh **Stream terrace deposits of the Rio Hondo (latest Pleistocene)**—Poorly sorted silt, sand, pebbles, cobbles, and boulders; clasts primarily of quartzite, schist, granite, and volcanic rock types; associated soils have stage I to II calcium carbonate development; typically present as thin (< 5 m) alluvial deposit on strath surfaces cut on volcanic bedrock or unit **QTl**; associated with the **Q6** surface of Kelson (1986).

Qt5rh **Stream terrace deposits of the Rio Hondo (late Pleistocene)**—Poorly sorted silt, sand, pebbles, cobbles, and boulders; clasts primarily of quartzite, schist, granite, and volcanic rock types; associated soils have stage II to III calcium carbonate development; typically present as thin (< 5 m) alluvial deposit on strath surfaces cut on volcanic bedrock or unit **QTl**; associated with the **Q5** surface of Kelson (1986).

Qt4rh **Stream terrace deposits of the Rio Hondo (middle? to late Pleistocene)**—Poorly sorted silt, sand, pebbles, cobbles, and boulders; clasts primarily of quartzite, schist, granite, and volcanic rock types; associated soils have stage III calcium carbonate development, argillic Bt soil horizons and 10YR to 7.5YR hues in Bt horizons;

typically present as thin (< 5 m) alluvial deposit on strath surfaces cut on volcanic bedrock or unit **QTl**; associated with the **Q4** surface of Kelson (1986).

Qt3rh **Stream terrace deposits of the Rio Hondo (middle? to late Pleistocene)**—Poorly sorted silt, sand, pebbles, cobbles, and boulders; clasts primarily of quartzite, schist, granite, and volcanic rock types; associated soils have stage III calcium carbonate development, argillic Bt soil horizons and 10YR to 7.5YR hues in Bt horizons.

Qt2rh **Stream terrace deposits of the Rio Hondo (middle? Pleistocene)**—Poorly sorted silt, sand, pebbles, cobbles, and boulders; clasts primarily of quartzite, schist, granite, and volcanic rock types; associated soils have stage III to IV calcium carbonate development, thick argillic Bt soil horizons, and 7.5YR to 10YR hues in soil Bt horizons; upper soil horizons are locally affected by surface erosion.

TERRACE DEPOSITS OF THE RED RIVER

Qt8rr **Stream terrace deposits of the Red River (middle to late Holocene)**—Poorly sorted silt, sand, pebbles, cobbles, and boulders; clasts primarily of quartzite, schist, granite, and volcanic rock types; deposits have negligible soil development; typically present as thin (< 5 m) alluvial deposit beneath high-stage floodplain or adjacent to active alluvial channels; equivalent to **Qt8** of Kelson (1986) and Pazzaglia (1989).

Qt7rr **Stream terrace deposits of the Red River (early to middle Holocene)**—Poorly sorted silt, sand, pebbles, cobbles, and boulders; clasts primarily of quartzite, schist, granite, and volcanic rock types; associated soils have stage I calcium carbonate development; typically present as thin (< 5 m) alluvial deposit on strath surfaces cut on volcanic bedrock; equivalent to **Qt7** of Kelson (1986) and Pazzaglia (1989).

Qt6rr **Stream terrace deposits of the Red River (latest Pleistocene)**—Poorly sorted silt, sand, pebbles, cobbles, and boulders; clasts primarily of quartzite, schist, granite, and volcanic rock types; associated soils have stage I to II calcium carbonate development; typically present as thin (< 5 m) alluvial deposit on strath surfaces cut on volcanic bedrock or unit **QTl**; associated with the **Q6** surface of Kelson (1986).

Qt5rr **Stream terrace deposits of the Red River (late Pleistocene)**—Poorly sorted silt, sand, pebbles, cobbles, and boulders; clasts primarily of quartzite, schist, granite, and volcanic rock types; associated soils have stage II to III calcium carbonate development; typically present as thin (< 5 m) alluvial deposit on strath surfaces cut on volcanic bedrock or unit **QTl**; associated with the **Q5** surface of Kelson (1986).

Qt4rr **Stream terrace deposits of the Red River (middle? to late Pleistocene)**—Poorly sorted silt, sand, pebbles, cobbles, and boulders; clasts primarily of quartzite, schist, granite, and volcanic rock types; associated soils have stage III calcium carbonate development, argillic Bt soil horizons and 10YR to 7.5YR hues in Bt horizons; typically present as thin (< 5 m) alluvial deposit on strath surfaces cut on volcanic bedrock or unit **QTl**; associated with the **Q4** surface of Kelson (1986).

Qt3rr **Stream terrace deposits of the Red River (middle? to late Pleistocene)**—Poorly sorted silt, sand, pebbles, cobbles, and boulders; clasts primarily of quartzite, schist, granite, and volcanic rock types; associated soils have stage III calcium carbonate development; typically present as thin (< 5 m) alluvial deposit on strath surfaces cut on volcanic bedrock or unit **QTl**; equivalent to **Qt3** of Kelson (1986) and Pazzaglia (1989).

Qt2rr **Stream terrace deposits of the Red River (middle? Pleistocene)**—Poorly sorted silt, sand, pebbles, cobbles, and boulders; clasts primarily of quartzite, schist, granite, and volcanic rock types; associated soils have stage III to IV calcium carbonate development; typically present as thin (< 5 m) alluvial deposit on strath surfaces cut on volcanic bedrock or unit **QTl**; includes correlative terrace deposit flanking the southwestern side of Lama Canyon on the Questa and Guadalupe Mountain quadrangles; equivalent to **Qt2** of Kelson (1986) and Pazzaglia (1989).

Qt1rr **Stream terrace deposits of the Red River (middle Pleistocene)**—Poorly sorted silt, sand, pebbles, and boulders; clasts of basalt, quartzite, metamorphic rock types, and volcanic rock types; soil development not documented but upper soil horizons are probably affected by surface erosion; present only locally along the rim of the Red River gorge, where **Qt1rr** is inset into **Qt0rr** gravel deposits and Tertiary volcanic rocks.

Qt0rr **Old stream terrace deposits flanking the Red River and tributaries (early? to middle? Pleistocene)**—Poorly sorted sand, pebbles, and cobbles; clasts of basalt, quartzite, and many volcanic and metamorphic rock types; the upper part is commonly affected by surface erosion; the unit is present upstream and downstream of the Red River Fish Hatchery and in the confluence area between the Rio Grande and the Red River; **Qt0rr** merges with unit **Qt0rg** in the southernmost part of the Guadalupe Mountain and Arroyo Hondo quadrangles.

SANTA FE GROUP

QTsf **Santa Fe Group, undivided (Miocene to early Pleistocene)**—In cross section only. Basin-fill clay, silt, sand, pebbles, cobbles, and boulders of the Rio Grande rift.

QTl **Lama formation (Pliocene to early? Pleistocene)**—Poorly sorted sand, pebbles, and cobbles; clasts of basalt, quartzite, other metamorphic rock types, and other volcanic rock types; locally high percentage of angular to subangular quartzite pebbles and cobbles; commonly cross-bedded, and stained with black manganese oxide and yellowish-orange iron oxide coatings; oxidized; clasts are typically weathered or grussified; contains distinct discontinuous sandy interbeds; commonly crudely imbricated; imbrication suggests westerly flow direction in area north of Taos Municipal Airport, and southerly flow direction in areas north and west of Rio Pueblo de Taos, with northwesterly flow direction in area southeast of Rio Pueblo de Taos; well drillers records in the Questa area show clay layers in the shallow subsurface that are interpreted as lacustrine deposits (Bauer et al., 2015); the unit is present between the Sangre de Cristo Mountains range front and the Rio Grande gorge over most of the map area; correlative with Lambert's (1966) two informal facies of the "Servilleta Formation" (the "sandy gravel facies" found south of the Rio Hondo, and the "gravelly silt facies" found between the Rio Hondo and the Red River); correlative with Kelson's (1986) informal "Basin Fill deposit;" correlative with the unit previously informally called "Blueberry Hill formation" in the Taos area; also correlative with Pazzaglia's (1989) late Neogene-Quaternary rift fill sequence (unit **Q1**) which he informally named the Lama formation; herein, for this study area, the Lama formation is defined as the uppermost, pre-incision, sedimentary rift fill, and where extant represents the uppermost member of the Santa Fe Group; the unit therefore includes all of the basin fill between the oldest Servilleta Basalt (40Ar/39Ar age of 5.55 ± 0.37 Ma near Cerro Azul, D. Koning, personal comm., 2015) and the oldest Rio Grande (and tributary) terrace gravels (e.g., **Qt0rg**, **Qt0rr**); the Lama formation and the underlying Chamita Formation are texturally and compositionally similar and may be indistinguishable in boreholes, although Koning et al. (2015) noted a coarsening of sediment (south of this map area) that roughly coincides with the Chamita/Lama contact in this map area; the top of the Lama formation is typically marked by a sharp unconformity and color/textural contrasts with overlying gravels; the unit contains several laterally variable components of sedimentary fill that are associated with various provenance areas related to east- or west-flowing tributary watersheds that have been fairly persistent in the late Cenozoic; locally contains tephra layers; reworked tephra in a road cut near the Red River Fish Hatchery (elevation ca. 7160 ft) was probably derived from nearby ca. 5

Ma volcanic units (R. Thompson, personal comm., 2015); a tephra in the uppermost Lama formation yielded a date of ~1.6 Ma based on a chemical correlation with the 1.61 Ma Guaje Pumice eruption in the Jemez Mountains (elevation ca. 7660 ft, M. Machette, personal comm., 2008); thickness ranges from zero to an exposed thickness of about 25 m at the southwestern end of Blueberry Hill, but may be considerably thicker in other parts of the map area.

Tcc **Clay layers in the Lama formation of the Santa Fe Group (Pliocene)**—In cross section only; boreholes east of Guadalupe Mountain have penetrated clay layers within the clastic beds of the Lama formation (**QTl**); composition and textures of clays are unknown, but they were likely deposited in short-lived lakes that developed behind lava dams along the ancestral Red River drainage; lateral continuity and extent are unknown; clays appear to influence the characteristics of groundwater flow systems by perching or mounding water above the regional aquifer, resulting in a locally elevated water table; layers are locally up to at least 100 feet thick.

Tc **Chamita Formation, undivided, Santa Fe Group (Miocene? and Pliocene)**—In cross section only. Sedimentary deposits between the lowest Servilleta Basalt and the Tesuque Formation; typically rounded to subrounded pebble- to cobble-size clasts in a sand to silt matrix; thick sections to the south reflect Proterozoic clast provenance and are dominated by schist, quartzite, and amphibolite with lesser volcanic clasts derived from the Latir volcanic field; locally, thin interbeds are typically dominated by pebble-size clasts in a fine sand to silt matrix and commonly includes the rock types above in addition to subangular and subrounded volcanic clasts derived locally from adjacent volcanic highlands of the Taos Plateau volcanic field; the top of **Tc** is herein defined as the sediments below the oldest Servilleta Basalt flows.

Tt **Tesuque Formation, Santa Fe Group (Miocene)**—In cross section only. Basin-fill deposits of clay, silt, sand, pebbles, cobbles, and boulders of the Rio Grande rift.

PICURIS FORMATION

Tp **Picuris formation, undivided (Oligocene to Miocene)**—In cross section only. In the Picuris Mountains area (Bauer, et al., 2017) this unit consists of an upper member of tuffaceous and pumiceous silty sandstones and volcaniclastic sandstone and conglomerate; a member of buff to white and/or pinkish, silty sandstone to fine cobble conglomerate and non-friable to strong, very fine lower to very coarse upper,

very poorly to moderately sorted, rounded to subangular, thinly to thickly bedded, silica-cemented silty to pebbly sandstone which locally contains a basal portion of poorly sorted pebbly/gravelly sandstone and/or cobble/boulder conglomerate composed exclusively of Proterozoic clasts; a member of light buff, yellowish, and locally white, ash-rich, quartzose, silty, fine sand to pebbly, pumiceous sandstone; a lower member of red, greenish, and yellowish, moderately to very poorly sorted, subangular to subrounded, pebbly/silty sandstone and mudstone containing very thick(?) to thin beds and/or lenses and/or isolated clasts of subangular to rounded Proterozoic quartzite (up to 3 m across) and massive quartzite conglomerate; paleoflow measurements near the Picuris Mountains indicate source to the north (Rehder, 1986; Aby et al., 2004); age range is from at least 35.6 Ma to less than 25 Ma; thickness unknown, but at least 450 m in the Picuris Mountains area.

ROCKS OF THE TAOS PLATEAU VOLCANIC FIELD

Tsb **Servilleta Basalt (Pliocene)**—Flows of dark-gray tholeiitic basalt characterized by small olivine and tabular plagioclase phenocrysts, diktytaxitic texture, and local vesicle pipes and segregation veins; forms thin, fluid, widespread pahoehoe basalt flows of the Taos Plateau volcanic field erupted principally from large shield volcanoes in the central part of the Taos Plateau (Lipman and Mehnert, 1979) but also from several small shields and vents to the northwest of the map area near the Colorado border (Thompson and Machette, 1989; K. Turner, personal comm., 2014); additional buried vents west of the Rio Grande likely exist; flows typically form columnar-jointed cliffs where exposed, with a maximum thickness of approximately 50 m in the Rio Grande gorge 16 km northwest of Taos; **Tsb** can locally be subdivided into the lower Servilleta Basalt (**Tsbl**), the middle Servilleta Basalt (**Tsbm**), and the upper Servilleta Basalt (**Tsbu**) that are separated by sedimentary intervals as much as 70 m thick in the southern part of the map area (Leininger, 1982); 40Ar/39Ar ages from basalts exposed in the Rio Grande gorge (Cosca et al., 2014) range in age from 4.78 ± 0.03 Ma for the lowest basalt near the Gorge Bridge, to 3.59 ± 0.08 Ma for the highest basalt flow at the Gorge Bridge, broadly consistent with previous results by Appelt (1998); the base of the upper Servilleta Basalt lava flow section at La Junta Point yielded an 40Ar/39Ar age of 3.78 ± 0.08 Ma (sample 10RG05 - M. Cosca, personal comm., 2014), whereas a lava flow at the base of the section south of Cerro Chiflo yielded an 40Ar/39Ar age of 3.78 ± 0.08 Ma (sample RT08GM02 - M. Cosca, personal comm., 2014).

Tsbu **Servilleta Basalt, upper (Pliocene)**—**Tsb** can locally be subdivided into the lower Servilleta Basalt (**Tsbl**), the middle Servilleta Basalt (**Tsbm**),

and the upper Servilleta Basalt (**Tsbu**) that are separated by sedimentary intervals as much as 70 m thick in the southern part of the map area (Leininger, 1982); 40Ar/39Ar ages from basalts exposed in the Rio Grande gorge (Cosca et al., 2014) range in age from 4.78 ± 0.03 Ma for the lowest basalt near the Gorge Bridge, to 3.59 ± 0.08 Ma for the highest basalt flow at the Gorge Bridge, broadly consistent with previous results by Appelt (1998); the base of the upper Servilleta Basalt lava flow section at La Junta Point yielded an 40Ar/39Ar age of 3.78 ± 0.08 Ma (sample 10RG05 - M. Cosca, personal comm., 2014), whereas a lava flow at the base of the section south of Cerro Chiflo yielded an 40Ar/39Ar age of 3.78 ± 0.08 Ma (sample RT08GM02 - M. Cosca, personal comm., 2014).

Tsbl **Servilleta Basalt, lower (Pliocene)**—**Tsb** can locally be subdivided into the lower Servilleta Basalt (**Tsbl**), the middle Servilleta Basalt (**Tsbm**), and the upper Servilleta Basalt (**Tsbu**) that are separated by sedimentary intervals as much as 70 m thick in the southern part of the map area (Leininger, 1982); 40Ar/39Ar ages from basalts exposed in the Rio Grande gorge (Cosca et al., 2014) range in age from 4.78 ± 0.03 Ma for the lowest basalt near the Gorge Bridge, to 3.59 ± 0.08 Ma for the highest basalt flow at the Gorge Bridge, broadly consistent with previous results by Appelt (1998); the base of the upper Servilleta Basalt lava flow section at La Junta Point yielded an 40Ar/39Ar age of 3.78 ± 0.08 Ma (sample 10RG05 - M. Cosca, personal comm., 2014), whereas a lava flow at the base of the section south of Cerro Chiflo yielded an 40Ar/39Ar age of 3.78 ± 0.08 Ma (sample RT08GM02 - M. Cosca, personal comm., 2014).

Tsbo **Older Servilleta Basalt (Pliocene)**—In cross section only. Identified in borehole BOR-6 and aeromagnetic data.

Tbo **Older Basalt (Miocene)**—In cross section only. Identified in borehole BOR-5 and aeromagnetic data.

Tdmc **Dacite of unnamed cerrito east of Montoso (UCEM) near-vent deposits (Pliocene)**—Near-vent deposits associated with lava flows of map unit **Tdm**; predominantly cinder, spatter agglutinate and local volcanic bombs.

Tdm **Dacite of unnamed cerrito east of Montoso (UCEM) (Pliocene)**—Dark gray, sparsely phyric, low-silica, calc-alkaline dacite (64 wt% Si02, 6 wt% Na20+K20) lava

flows erupted from two vent areas east of Cerro Montoso; contains rare skeletal pyroxene phenocrysts and resorbed, subhedral olivine and quartz xenocrysts in a microcrystalline to glassy groundmass; locally includes small volume, aerially restricted andesite flows (McMillan and Dungan, 1986); 40Ar/39Ar age determinations of 4.08 ± 0.04 Ma (sample 11RG42) and 4.6 ± 0.02 Ma (sample 11RG27) from north and south UCEM areas respectively (M. Cosca, personal comm., 2014); Appelt (1998) reported a similar 40Ar/39Ar age determination of 4.11 ± 0.13 Ma from a northern UCEM exposure; UCEM locally caps the west rim of the Rio Grande gorge, forming a thin veneer that is typically a single flow thickness over the Servilleta Basalt (unit **Tsbu**) and local interbedded sedimentary deposits (Leininger, 1982; Peterson, 1981); these relations are not shown at the scale of this map due to the extensive landslide deposits (unit **Qls**); scoria and spatter agglutinate are common near the poorly defined vent areas.

Tvr **Volcanic deposits of the Red River volcano (Pliocene)**—Dacite lava flows and near-vent pyroclastic deposits of moderate relief on the south side of Guadalupe Mountain and in-canyon exposures in the middle and upper reaches of the Red River where dacite lava flows cap the gorge sequence on both sides of the drainage; the lava flows exposed on both sides of the Red River were fed locally by dikes exposed on both sides of the canyon; McMillan and Dungan (1986) reported chemical compositions for the underlying basaltic andesite (unit **Tvhc**) to dacite suite ranging from 52 to 61 wt% SiO2 and from 4.2 to 7.4 wt% Na2O+K2O; medium-grey dacite lavas are porphyritic, containing 5-15% phenocrysts of augite and bronzite with common olivine xenocrysts in a fine-grained to glassy groundmass of plagioclase, glass, pyroxenes, and titanomagnetite (McMillan and Dungan, 1986); dacite lavas are typically thick, up to tens of meters locally, and are characteristically discontinuous and aerially restricted; deposits of the Red River volcano overlie andesitic lava flows of the Hatchery volcano (unit **Tvh**) and locally deposits of south Guadalupe Mountain (unit **Tdgs**); 40Ar/39Ar age determination of 4.67 ± 0.06 Ma (sample RT08GM12 - M. Cosca, personal comm., 2014) was obtained from a sample collected near the northeastern limit of exposed deposits.

Tv **Basalt (Pliocene?)**—Basalt.

Tvh **Volcanic deposits of Hatchery volcano (Pliocene)**—Includes a sequence of lava flow, intercalated volcanic breccia, and near vent pyroclastic deposits in canyon exposures in the middle and upper reaches of the Red River drainage and as low relief hills adjacent to the Red River; lava flows include a series of predominantly basaltic andesite and andesite lava flows; McMillan and Dungan (1986) reported chemical compositions for the basaltic andesite to overlying dacite (unit **Tvr**) ranging

from 52 to 61 wt% SiO2 and from 4.2 to 7.4 wt% Na2O+K2O; dark gray basaltic andesite and andesite lava flows typically contain 5-10% phenocrysts of olivine and plagioclase; olivine phenocrysts can be large (up to 6mm) exhibiting well-developed skeletal overgrowths (McMillan and Dungan, 1986); andesite lava flows with aa flow tops and well exposed basal flow breccias tend to be thin, a few meters to 10 m thick, and are laterally continuous based on exposures in the Red River canyon; deposits of the Hatchery volcano overlie dacite lava flows of Guadalupe Mountain, and locally overly two lava flows of Servilleta Basalt at the base of the Red River gorge near the New Mexico State Fish Hatchery (not differentiated at the map scale); 40Ar/39Ar age determination of 4.82 ± 0.07 Ma (sample 11RG42 - M. Cosca, personal comm., 2014) was obtained from a sample at the base of the section approximately 0.6 km southwest of the New Mexico State Fish Hatchery.

Tvhc **Volcanic deposits of the Hatchery volcano, near vent (Pliocene)**—Near-vent deposits associated with lava flows of map unit **Tvh**; predominantly cinder, spatter, and agglutinate exposed in the Red River drainage approximately 1.25 km northwest of the New Mexico State Fish Hatchery; near-vent spatter, agglutinate, and volcanic bombs are common near hill 7590′ on the south side of the Red River.

Tao **Andesite of Cerro de la Olla (Pliocene)**—Dark gray to black, porphyritic, olivine andesite (58.5 wt% SiO2, 6.9 wt% Na20+K20) lava flows that erupted from vents near the summit of Cerro de la Olla, one of the largest, petrologically uniform, shield volcanoes of the Taos Plateau volcanic field (Lipman and Mehnert, 1979); contains 2-3% phenocrysts of olivine in a microcrystalline groundmass of plagioclase, olivine, augite, Fe-Ti oxides; the lower slopes of Cerro de la Olla in the northwestern part of the map area are commonly mantled in colluvium and rarely preserve well-developed flow morphology; instead outcrops typically exhibit blocky flow tops and remnants of numerous discontinuous and aerially restricted flow lobes; Appelt (1998) reported an 40Ar/39Ar age of 4.97 ± 0.06 Ma for a groundmass separate from the west side of Cerro de la Olla.

Tdgn **Dacite of Guadalupe Mountain, north (Pliocene)**—Predominantly trachydacite lava flows (62 wt% SiO2, 6.3 wt% Na20+K20) and associated near-vent pyroclastic deposits; contains sparse, small phenocrysts of plagioclase, hypersthene, and augite in a pilotaxitic glassy groundmass; proximal lava flows, lava dome remnants, and near-vent pyroclastic deposits consisting mostly of spatter and agglutinate of the geographic north peaks of Guadalupe Mountain; spatter and cinder deposits are found locally in association with flank lavas and may represent remobilized central vent deposits or mark the location of satellite vents on the flanks of north Guadalupe

Mountain; distinguished from lava flows of south Guadalupe Mountain on the basis of reversed magnetic polarity based on paleomagnetic and aeromagnetic determinations (M. Hudson and V.J.S. Grauch respectively, personal comm., 2014; Grauch et al., 2015; Bauer et al., 2015); 40Ar/39Ar age determination of 5.04 ± 0.04 Ma (sample 10RG06 - M. Cosca, personal comm., 2014).

Tdgs **Dacite of Guadalupe Mountain, south (Pliocene)**—Predominantly trachydacite lava flows (62 wt% SiO2, 6.3 wt% Na20+K20) and associated near-vent pyroclastic deposits; contains sparse, small phenocrysts of plagioclase, hypersthene, and augite in a pilotaxitic glassy groundmass; proximal lava flows, lava dome remnants, and near-vent pyroclastic deposits consisting mostly of spatter and agglutinate of the geographic south peaks of Guadalupe Mountain; distinguished from lava flows of north Guadalupe Mountain on the basis of reversed magnetic polarity based on paleomagnetic and aeromagnetic determinations (M. Hudson and V.J.S. Grauch respectively, personal comm., 2014; Grauch et al., 2015; Bauer et al., 2015); 40Ar/39Ar age determination of 5.00 ± 0.04 Ma (sample 10RG07 - M. Cosca, personal comm., 2014); stratigraphic position relative to unit **Tdgn** is based on geophysical modeling of aeromagnetic data (B. Drenth, V.J.S. Grauch, personal comm., 2014) and age constraints relative to geomagnetic time scale; Appelt (1998) reported 40Ar/39Ar ages of 5.11 ± 0.08 Ma and 5.34 ± 0.06 Ma for groundmass separates from the south side of Guadalupe Mountain.

Tdg **Dacite of Guadalupe Mountain, undivided (Pliocene)**—Predominantly trachydacite lava flows (62 wt% SiO2, 6.3 wt% Na20+K20); contains sparse, small phenocrysts of plagioclase, hypersthene, and augite in a pilotaxitic glassy groundmass; distal lava flows exposed in the Rio Grande gorge and the Red River gorge are highly elongate and individual flows are laterally restricted, typically forming overlapping finger-like lobes characterized by radial cooling fractures and concentric brecciated carapaces where exposed in cross section; flows exposed in the Rio Grande gorge range considerably in thickness from a few meters to several tens of meters; lava flow directions exposed in the Rio Grande gorge appear to be predominantly from east to west, suggesting a primary source area at Guadalupe Mountain; dacite lava flows overlie both Cerro Chiflo dome deposits and lower Servilleta Basalt lava flows in the Rio Grande gorge; 40Ar/39Ar age determination of 5.27 ± 0.05 Ma (sample 11RG08 - M. Cosca, personal comm., 2014).

Tdcn **Dacite of Cerro Negro (Miocene)**—Dark gray to black, extensively fractured, two-pyroxene dacite; yielded an 40Ar/39Ar age of approximately 5.7 Ma (McIntosh et al., 2004).

Tam **Andesite of Cerro Montoso (Miocene)**—Dark gray to black, porphyritic, olivine andesite (57.6 wt% SiO2, 8 wt% Na20+K20) lava flows erupted from vents on Cerro Montoso, one of the largest, petrologically uniform, shield volcanoes of the Taos Plateau volcanic field (Lipman and Mehnert, 1979); contains 2-3% phenocrysts of olivine in a microcrystalline groundmass of plagioclase, olivine, augite, and Fe-Ti oxides; the lower slopes of Cerro Montoso in the western map area are commonly mantled in colluvium, and rarely preserve well-developed flow morphology; instead outcrops typically exhibit blocky flow tops and remnants of many discontinuous and aerially restricted flow lobes; Appelt (1998) reported an 40Ar/39Ar age of 5.88 ± 0.18 Ma for a groundmass separate from the west side of Cerro Montoso.

Tvc **Trachyandesite of Cerro Chiflo (Miocene)**—Eroded remnants of large lava dome of porphyritic trachyandesite (63 wt% SiO2, 7.7 wt% Na2O+K2O; rock designation based on IUGS classification (Le Bas et al., 1986); formerly described by Lipman and Mehnert (1979) as quartz latite; forms prominent cliff outcrops along the Rio Grande gorge in the northern part of the map area; light brown to gray, weakly to strongly flow laminated, with phenocrysts of plagioclase, hornblende, and sparse biotite in a devitrified groundmass; xenoliths of Proterozoic schist, gneiss, and granite are common; flow breccias preserved around the margins of dome and ramp structures are common throughout the exposed interior; Appelt (1998) reported 40Ar/39Ar ages of 5.31 ± 0.31 Ma and 5.32 ± 0.08 Ma for groundmass separates from the west and east sides of the dome, respectively; more recently, preliminary 40Ar/39Ar total fusion age determinations of 10.65 Ma and 9.86 Ma on biotite and hornblende separates, respectively (sample 11RG43 - M. Cosca, personal comm., 2014), are more consistent with previously determined Miocene potassium-argon ages reported by Lipman and Mehnert (1979).

EARLY-RIFT VOLCANIC & VOLCANICLASTIC ROCKS

Tvb **Volcanic deposits of Brushy Mountain (Oligocene)**—Volcanic rocks and deposits consisting primarily of andesite to dacite lava flows and flow breccias and rhyolite block-and-ash flows and ash-flow tuff with volumetrically minor air-fall deposits (Thompson et al., 1986; Thompson and Schilling, 1988). Light tan, poorly welded, lithic-rich, rhyolite ash-flow tuff forms the base of the section near the low saddle of

Brushy Mountain; the lower rhyolite contains phenocrysts of plagioclase and altered biotite, light brown altered pumice and angular to subangular vitrophyric inclusions (<0.5 cm to several cm) containing plagioclase phenocrysts and reddish-brown dacite inclusions (2 cm to several cm); locally overlain by thin outflow deposits of Amalia Tuff (unit **Tat**); post-Amalia Tuff deposits include light-grey to white rhyolite dome deposits including locally, block-and-ash flows, ash-flow tuffs, and air-fall deposits; all deposits are mineralogically similar, containing sanidine, quartz, and minor biotite phenocrysts in a devitrified glass matrix; exposed in the quarry on the south side of Brushy Mountain and the north side of Cerro Montoso; thin (< 2-3 m) andesite lava flows locally overlie rhyolite dome deposits and consist of medium- to dark-brown, porphyritic flows and flow remnants containing olivine, clinopyroxene, and plagioclase phenocrysts, plagioclase glomerocrysts, and minor orthopyroxene microphenocrysts in a fine- to medium-grained trachytic groundmass composed predominantly of plagioclase, clinopyroxene, and Fe-Ti oxides; the upper part of the section consists of light- to dark-gray, aphyric to porphyritic, dacite lava flows and flow breccias containing variable amounts of hornblende, plagioclase, clinopyroxene, Fe-Ti oxides, and minor orthopyroxene, sanidine, sphene, and zircon in a fine-grained to microcrystalline groundmass; lava flows are locally variable in thickness, discontinuous and commonly delineated on the basis of blocky rubble deposits and float; in the Rio Grande gorge, deposits are dominantly andesite to dacite breccias and reworked pyroclastic deposits overlying biotite- and hornblende-bearing dacite lava flows; Zimmerer and McIntosh (2012) reported 40Ar/39Ar age determination of 25.17 ± 0.04 Ma on sanidine from a basal rhyolite of the Brushy Mountain section, and 22.69 ± 0.08 Ma from groundmass concentrates from an andesite lava flow in the upper part of the section.

Tvt **Volcanic deposits of Timber Mountain (Oligocene)**—Volcanic rocks and deposits consisting primarily of andesite to dacite lava flows and flow breccias and lesser rhyolite flows and ash-flow tuff (Thompson et al., 1986; Thompson and Schilling, 1988); light-brown, lithic-poor, densely welded, rhyolite ash-flow tuff forms the base of the section and contains moderately to highly flattened pumices, phenocrysts of plagioclase, sanidine, quartz, and biotite with subordinate amounts of Fe-Ti oxides, clinopyroxene, and orthopyroxene in a glassy to partially devitrified matrix; rhyolite ash-flow tuff is overlain by a lower sequence of moderately porphyritic lava flows and pyroclastic deposits containing variable amounts of plagioclase, clinopyroxene, Fe-Ti oxides, hornblende, plus or minus biotite, and sanidine xenocrysts; locally contains abundant micropillows of basaltic lava and dacite xenoliths as much as 10 cm in diameter; lower dacite sequence is separated from an upper dacite sequence locally by medium- to dark-brown, porphyritic lava flow remnants containing

olivine, clinopyroxene, and plagioclase phenocrysts, plagioclase glomerocryts, and minor orthopyroxene microphenocrysts in a fine- to medium-grained trachytic groundmass composed of plagioclase, clinopyroxene, and Fe-Ti oxides; upper dacite sequence contains medium- to light-gray porphyritic, glassy lava flows and lava dome remnants containing phenocrysts of hornblende, biotite, plagioclase, clinopyroxene, and Fe-Ti oxides in variable proportion; a whole rock 40Ar/39Ar age of 24.22 ± 0.12 Ma (M. Cosca, personal comm., 2014) was obtained from a basal dacite vitrophyre southwest of the map area.

ROCKS OF THE QUESTA MAGMATIC SYSTEM

VOLCANIC

Tqi **Latite and quartz latite (Miocene and Oligocene)**—Light tan to gray latite and quartz latite, often stained rust brown, with 15-30% phenocrysts of sanidine, pyroxene and/or hornblende, sparse quartz, and altered cubes of pyrite; plagioclase phenocrysts to several centimeters in length are present; occurs as dikes up to 20 m wide and elongate intrusive masses north of the D.H. Lawrence Ranch (Lipman and Read, 1989).

Tri **Aphanitic rhyolite (Miocene and Oligocene)**—Aphanitic to sparsely porphyritic rhyolite, otherwise similar to **Trp** (Lipman and Read, 1989).

Trpp **Peralkaline rhyolite (Miocene and Oligocene)**—Dikes and irregular intrusions of alkali rhyolite and granite porphyry (76-77% SiO2) chemically similar to the Amalia Tuff (**Tat**) and associated caldera-related rhyolitic lava flows; contains 1-25% phenocrysts of quartz and sodic alkali feldspar; locally contains small phenocrysts of arfvedsonite and acmite, especially in the caldera-margin ring dike along Jaracito Canyon and in the Virgin Canyon-Virsylvia Peak area, where the peralkaline rhyolite forms marginal facies of metaluminous biotite-bearing intrusions of granite porphyry within the caldera; dated by K-Ar and F-T methods at about 26 Ma (Lipman and Read, 1989).

Trp **Porphyritic rhyolite (Miocene and Oligocene)**—White to light tan to light gray porphyritic rhyolite typically containing 5-20% phenocrysts of quartz, sanidine, and sparse plagioclase and biotite; occurs as dikes 1-10 m wide and local irregular and shallow intrusions (Lipman and Read, 1989); generally only observed as float.

Tqk **Potassium feldspar quartz latite (Miocene and Oligocene)**—Coarsely porphyritic, light-gray quartz latite containing potassium feldspar phenocrysts as long as 5 cm (Lipman and Read, 1989).

Tapi **Porphyritic andesite and dacite (Miocene and Oligocene)**—Fine-grained, dark gray, aphanitic and porphyritic andesite and minor basalt; where present, phenocrysts include hornblende, plagioclase, biotite, and little or no quartz or sanidine (Lipman and Read, 1989).

Tu **Tertiary rocks along the Sangre de Cristo fault, undivided (Miocene and Oligocene)**—Rocks related to the Questa magmatic system that are undivided along the Sangre de Cristo fault zone; these units were mapped as Quaternary deposits by Lipman and Read (1989), but are herein mapped as unknown bedrock that is generally covered by surficial deposits that are too thin to delineate as map units.

Tat **Amalia Tuff (Oligocene)**—Light gray to light brown moderately welded porphyritic, peralkaline, rhyolite ash-flow tuff erupted from the Questa caldera just east of the Village of Questa (Lipman and Reed, 1989); consists primarily of quartz and sanidine phenocrysts in a devitrified matrix; Fe-Ti oxides, titanite, and alkali amphibole phenocrysts are minor, lithic fragments are common; forms low erosional hills of outflow near Brushy Mountain in the Guadalupe Mountain quadrangle; Zimmerer and McIntosh (2012) reported a mean age of 25.39 ± 0.04 Ma based on 13 40Ar/39Ar laser fusion analyses of Amalia Tuff.

Tatl **Lithic-rich lower facies of Amalia Tuff (Oligocene)**—Non-welded to partly welded tuff up to 30 m thick, containing as much as 5% fragments of andesitic volcanic rocks; sparse fragments of Proterozoic rocks present locally; generally grades upward into main unit; locally difficult to distinguish from older tuff of Tetilla Peak (**Ttp**) (Lipman and Reed, 1989).

Tq **Lava flows and domes (Oligocene)**—Massive quartz latite, locally flow layered; commonly gray to greenish gray, especially where propylitically altered in interiors of thick flows; tops of less altered flows are light red-brown or light gray; intrusive quartz latite (**Tqi**) locally is difficult to distinguish from flow rocks; maximum thickness is at Latir Mesa, where sections through seemingly single flows or domes exceed 500 m (Lipman and Read, 1989).

Ta **Andesitic lava flows (Oligocene)**—Purplish-gray to gray, aphanitic to porphyritic andesite lava flows and flow breccias, with minor interbedded volcaniclastic sediments; phenocrysts include plagioclase and hornblende (Lipman and Read, 1989).

Trc **Rhyolite of Cordova Creek (Oligocene)**—Light-tan to light-gray rhyolitic lava flows and domes (74-77% SiO2) containing about 5% phenocrysts of quartz, alkali feldspar, plagioclase, and biotite; commonly massive and devitrified; locally flow laminated; large domes centered at Cordova Creek, Van Diest Peak, and Italian Creek also appear to be sources for main accumulations of tuff of Tetilla Peak; as thick as 250 m at head of Cordova Creek (Lipman and Read, 1989).

Ttp **Tuff of Tetilla Peak (Oligocene)**—Quartz-rich, light-colored, weakly welded, rhyolitic ash-flow tuff containing abundant small volcanic fragments; contains 10-30% phenocrysts of quartz, sanidine, plagioclase and sparse chloritized biotite; lithic fragments mostly andesite and quartz-bearing rhyolite (Lipman and Read, 1989).

PLUTONIC

Tgy **Lucero Peak pluton (Miocene)**—White to pale pink, medium to coarse grained equigranular granite to quartz monzonite (Lipman and Read, 1989).

Tgb **Biotite granite (Oligocene)**—Granitic roof phase of the Rio Hondo pluton emplaced in the Questa caldera at about 26 Ma, during volcanism and caldera formation; medium-grained and equigranular, with sparse aplite and no hornblende (Lipman and Read, 1989).

Tgp **Granite porphyry (Oligocene)**—Fine-grained porphyritic biotite granite and aplite, texturally transitional between mapped bodies of granite (**Tgb**) and intrusive porphyritic rhyolite (**Trp**) or rhyolite (**Tri**), especially in the Rito del Medio and Canada Pinabete areas (Lipman and Read, 1989).

Tgd **Rio Hondo pluton (Oligocene)**—White to pale, grayish-orange, medium- to fine-grained, massive to locally foliated granodiorite; white to pale orange, aphanitic-porphyritic border facies has quartz phenocrysts and local breccia; has potassium feldspar phenocrysts up to 4 cm in size; generally forms rounded outcrops with abundant grus (Lipman and Read, 1989).

SEDIMENTARY

Tvs **Volcanic sedimentary rocks (Oligocene)**—Relatively well-bedded and well-sorted volcanic sedimentary rocks of andesitic to rhyolitic composition at many levels in the volcanic sequence; dominantly fluviatile and deltaic deposits; the volcanic sedimentary rocks are locally tuffaceous and interfinger and intergrade in places with the tuff of Tetilla Peak (**Ttp**); also included are local air-fall and reworked silicic tuff underlying the Amalia Tuff (**Trt**); exposed thickness nowhere more than about 50 m (Lipman and Read, 1989).

Tps **Prevolcanic sedimentary rocks (Lower Oligocene or Eocene)**—Discontinuous lenses of weakly indurated shale, sandstone, and conglomerate derived from Proterozoic sources; commonly expressed mainly by reddish-brown silty soil; cobbles of green quartzite are locally distinctive; outcrops rare, except where baked near granitic intrusion along the Red River; indurated Tertiary sedimentary rocks, which have been correlated with Permian and Pennsylvanian Sangre de Cristo Formation (McKinlay, 1957; Clark and Read, 1972), occur only within areas of Tertiary thermal metamorphism and lack limestone interbeds characteristic of the Sangre de Cristo in adjacent areas; probably correlative with the Vallejo Formation of Upson (1941) in the Sangre de Cristo Mountains in southern Colorado, and with the Blanco Basin Formation and Telluride Conglomerate in the San Juan Mountains; thickness 0-100 m (Lipman and Read, 1989).

SEDIMENTARY DEPOSITS OF THE TAOS TROUGH

IPu **Sedimentary rocks of the Taos Trough, undivided (Pennsylvanian)**—Poorly exposed; greenish, reddish, yellowish, buff, tan, black, and brown; very friable-to-firm; sandy to clayey; thinly to thickly bedded; poorly to moderately well-cemented(?), sandy to clayey siltstone, mudstone, and shale interbedded with mostly greenish and brownish, firm to very strong, poorly to moderately well-sorted, poorly to moderately well rounded, thin- to very thickly bedded, moderately to very well-cemented, quartzose, feldspathic, and arkosic, silty to pebbly sandstone and sandy conglomerate and less common thin- to thick-bedded, grayish and blackish limestone of the Alamitos and Flechado Formations; contains a rich assortment of fossils; sandstones commonly contain plant fragments that have been altered to limonite(?); contacts between beds are generally sharp, rarely with minor scour (less than ~20 cm); the lower contact is not exposed in the map area, although to the south, the lower contact is mapped at the top of the Del Padre Sandstone or highest

Mississippian carbonate, or at the base of the lowest sedimentary bed where Mississippian rocks are absent; conglomeratic layers in the lower part of the unit locally contain rare, sometimes banded, chert pebbles; equivalent to the Sandia, Madera, and La Posado Formations to the south; fusulinids collected in the Taos quadrangle are Desmoinesian in age (Bruce Allen, personal comm., 2000); may locally contain minor amounts of Mississippian strata; Miller et al. (1963) measured an incomplete section of 1756 m along the Rio Pueblo near the Comales Campground, and an aggregate thickness of Pennsylvanian strata of >1830 m.

IPcq **Conglomerate (Pennsylvanian)**—Lenses of quartzite pebble/boulder, clast-supported conglomerate with sandy matrix; clasts average about 6 inches in diameter, although some are greater than 2 feet; rounded to well-rounded; very poorly sorted; thickness ranges up to several meters.

IPlst **Limestone (Pennsylvanian)**—Light gray limestone in scattered, discontinuous layers; fossiliferous to non-fossiliferous; fossils include phylloid algae, crinoids, brachiopods, and other shell fragments; well bedded to poorly bedded; outcrops are typically highly weathered, and locally are highly fractured; limestone represents a very small percentage (<1%) of the volume of Pennsylvanian rock in the map area.

IPss **Sandstone (Pennsylvanian)**—Medium-grained to very coarse-grained sandstone; tan to gray; poorly sorted to well sorted; typically non-calcareous; locally contains lenses of conglomerate composed mainly of quartzite pebbles; locally contains wood chips and plant fossils (possibly ferns); thickness ranges from less than a meter to tens of meters.

METAMORPHIC ROCKS OF THE SANGRE DE CRISTO MOUNTAINS

Tu & XYu **Bedrock units of Sangre de Cristo Mountains (Miocene to Proterozoic)**—In cross section only. Bedrock units of Sangre de Cristo Mountains have been combined to form a single unit for the purposes of the cross section. This represents undivided Tertiary rocks along the Sangre de Cristo fault (**Tu**) and Proterozoic rocks (**XYu**).

XYu **Proterozoic rocks, undivided (Paleoproterozoic and Mesoproterozoic)**—Supracrustal metamorphic rocks and plutonic and metaplutonic rocks; shown in cross sections and on Taos Pueblo lands that remain unmapped.

METASEDIMENTARY

Xq **Quartzite (Paleoproterozoic)**—White to gray, massive, vitreous quartzite with crossbeds defined by heavy mineral concentrations; pervasively fractured into decimeter-scale, angular lozenges by joints, irregular fractures, and bedding (Lipman and Read, 1989); the map includes the unpublished, detailed mapping of J. Grambling (Univ. of New Mexico, personal comm., 1991) in the San Cristobal Canyon and Cerrito Colorado areas, which supersedes the work of Lipman and Read (1989).

Xms **Biotite muscovite schist and gneiss (Paleoproterozoic)**—Medium- to coarse-grained, thinly layered to massive, lustrous, quartz-mica schist and gneiss; commonly contains sillimanite; locally contains garnet, andalusite, and cordierite (Lipman and Read, 1989).

Xlg **Layered gneiss (Paleoproterozoic)**—Conspicuously layered and well-foliated, fine- to medium-grained, biotite gneiss, biotite-hornblende gneiss, hornblende gneiss, and amphibolite; rocks consist of various proportions of quartz, oligoclase-andesine, blue-green hornblende, brown biotite, epidote, and magnetite; layers range in thickness from a few centimeters to several meters and commonly display rootless isoclinal fold noses and variations in thickness due to ductile deformation; thin lenses and layers of ferruginous quartzite, magnetite ironstone, and quartz-epidote-calcite marble are commonly interleaved; compositions suggest that many of the layers could have been derived from intermediate volcanic or volcaniclastic rocks; local graded bedding suggests derivation from graywackes, perhaps with a significant volcanic component (Lipman and Read, 1989).

METAVOLCANIC

Xfg **Felsic gneiss (Paleoproterozoic)**—Pale gray to orange-brown, micaceous, weakly to moderately foliated, quartzofeldspathic gneiss locally grading to micaceous quartzite; commonly interlayered with amphibolite and amphibole gneiss (Lipman and Read, 1989).

Xa **Amphibolite (Paleoproterozoic)**—Thinly layered to massive, fine- to coarse-grained, medium green to dark green to black amphibolite and amphibole gneiss; locally contains calc-silicate gneiss, biotite-hornblende gneiss, felsic gneiss, and muscovite biotite schist (Lipman and Read, 1989).

Xcg **Metaconglomerate (Paleoproterozoic)**—Composed of closely packed 0.5-4-cm angular to subrounded white, blue-gray, and red-brown quartz pebbles in a fine-grained arkosic matrix; interlayered with muscovitic felsic gneiss south of Lama Canyon (Lipman and Read, 1989).

Xvf **Felsic metavolcanic rocks (Paleoproterozoic)**—Fine-grained, light gray, greenish-gray, or pink, massive to strongly foliated, felsic, blastoporphyritic gneiss containing conspicuous 2-5-mm ovoid grains of bluish-gray quartz and 1- to 5-mm laths of white feldspar; groundmass consists of a microcrystalline mosaic of quartz, plagioclase, K-feldspar, epidote, and scattered flakes of biotite; feldspar porphyroblasts include both plagioclase (oligoclase) and grid-twinned microcline with irregular blotches of albite; composition is similar to rhyolite or rhyodacite; widespread layering and local graded bedding show that a large part of the unit is derived from tuffs or volcaniclastic rocks; zircon from volcaniclastic rock northeast of Gold Hill yielded an upper-intercept concordia age of 1,765 Ma (Lipman and Read, 1989).

METAPLUTONIC

Xqc **Quartz monzonite of Columbine Creek (Paleoproterozoic)**—White to gray to pale tan, moderately to strongly foliated quartz monzonite; recrystallized to sugary textured, non-foliated rock near Tertiary plutons; age is 1730 Ma (Lipman and Reed, 1989).

Xmi **Mafic and ultramafic rocks (Paleoproterozoic)**—Medium- to coarse-grained dark-green to greenish-gray weakly foliated gabbro and serpentinized ultramafic rocks; gabbro consists of equant clots of hornblende in a matrix of calcic plagioclase, epidote, and sparse quartz; in smaller bodies the gabbro is medium to fine grained, distinctly foliated, and displays chilled margins; original ophitic or intergranular textures are locally preserved and a few bodies display relict cumulus layering; ultramafic rocks are similar to gabbro, except that quartz is absent and plagioclase sparse; mapped only where intrusive into supracrustal rocks; similar rocks are widespread as inclusions in plutonic rocks where they are mapped as amphibolite (**Xa**); age of most bodies undetermined, but zircon from gabbro sill west of Gold Hill yielded an upper-intercept concordia date of 1741 Ma, interpreted as the emplacement age (Lipman and Read, 1989).

Xtr **Tonalite of Red River (Paleoproterozoic)**—Gray to green, medium- to coarse-grained, strongly foliated, biotite-hornblende tonalite (quartz diorite); consists of a mosaic of recrystallized quartz, plagioclase, and biotite studded with 0.5- to 1-cm ovoid porphyroclasts of faintly zoned andesine; hornblende forms large irregular sieve-textured grains and scattered small grains in the mosaic; locally grades into gabbro; slabs and blocks of layered gneiss are locally abundant as inclusions; zircon from tonalite along road to Middle Fork Lake gives an upper-intercept concordia date of 1,750 Ma, interpreted as the emplacement age (Lipman and Read, 1989).

References

Aby, S.B., 2008, Geologic Map of the Servilleta Plaza quadrangle, Taos County, New Mexico: New Mexico Bureau of Geology and Mineral Resources Open-File Geologic Map Open-file Geologic Map 182, scale 1:24,000.

Aby, S.B., Bauer, P.W., and Kelson, K.I., 2004, The Picuris Formation: A late Eocene to Miocene sedimentary sequence in northern New Mexico, in Brister, B.S, Bauer, P.W., Read, A.S., and Lueth, V.W., eds., Geology of the Taos Region: New Mexico Geological Society 55th Annual Field Conference, p. 335-350.

Appelt, R.M., 1998, $^{40}Ar/^{39}Ar$ geochronology and volcanic evolution of the Taos Plateau volcanic field, northern New Mexico and southern Colorado [M.S. thesis]: Socorro, New Mexico Institute of Mining and Technology, 58 p.

Bauer, P.W., and Kelson, K.I., 2001, Geologic map of the Taos quadrangle, Taos County, New Mexico: New Mexico Bureau of Geology and Mineral Resources Open-File Geologic Map OF-GM 43, scale 1:24,000.

Bauer, P.W., Kelson, K.I., Aby, S.B., Helper, M., and Mansell, M.M., 2017, Geologic map of the Picuris Mountains region, Taos and Rio Arriba Counties, New Mexico, New Mexico Bureau of Geology and Mineral Resources Open-File Geologic Map 294, scale 1:24,000.

Bauer, P.W., Johnson, P.S., Grauch, T., Drenth, B., and Thompson, R.A., 2015, Hydrogeologic cross sections of the Questa area, Taos County, New Mexico: Final Technical Contract Report for the Village of Questa, New Mexico Bureau of Geology and Mineral Resources, Open-File Report 578, 13 p. plus plates and appendices.

Clark, K. F., and Read, C. B., 1972, Geology and ore deposits of Eagle Nest area, New Mexico: New Mexico Bureau of Mines and Mineral Resources Bulletin 94, 162 p.

Cosca, M., Thompson, R., and Turner, K., 2014, High precision $^{40}Ar/^{39}Ar$ geochronology of Servilleta Basalts of the Rio Grande gorge, New Mexico: Abstract V51A-4728 presented at 2014 Fall Meeting, AGU, San Francisco, California, 15-19 December.

Galusha, T., and Blick, J.C., 1971, Stratigraphy of the Santa Fe Group, New Mexico: American Museum of Natural History Bulletin 144, 127 p.

Grauch, V.J.S., Drenth, B.J., Thompson, R.A., and Bauer, P.W., 2015, Preliminary geophysical interpretations of regional subsurface geology near the Questa Mine Tailing Facility and Guadalupe Mountain, Taos County, New Mexico: U.S. Geological Survey Open-File Report 2015–1129, 35 p., http://dx.doi.org/10.3133/ofr20151129.

Kelson, K.I., 1986, Long-term tributary adjustments to base level lowering in northern Rio Grande rift, New Mexico [M.S. thesis]: Albuquerque, University of New Mexico, 210 p.

Kelson, K.I. and Bauer, P.W., 2003, Geologic map of the Los Cordovas 7.5-minute quadrangle, Taos County, New Mexico: New Mexico Bureau of Geology and Mineral Resources Open-File Geologic Map OF-GM 63, scale 1:24,000.

Kelson, K.I. and Bauer, P.W., 2006, Geologic map of the Arroyo Hondo 7.5-minute quadrangle, Taos County, New Mexico: New Mexico Bureau of Geology and Mineral Resources Open-File Geologic Map OF-GM 116, scale 1:24,000.

Kelson, K.I., Thompson, R.A., and Bauer, P.W., 2008, Geologic map of the Guadalupe Mountain 7.5-minute quadrangle, Taos County, New Mexico: New Mexico Bureau of Geology and Mineral Resources Open-File Geologic Map OF-GM 168, scale 1:24,000.

Kelson, K.I., Bauer, P.W., and Rawling, G., 2010, Geologic map of the Arroyo Seco 7.5-minute quadrangle, Taos County, New Mexico: New Mexico Bureau of Geology and Mineral Resources Open-File Geologic Map OF-GM 170, scale 1:24,000.

Kelson, K.I., Bauer, P.W., and Thompson, R.A., 2013, Geologic map of the Questa 7.5-minute quadrangle, Taos County, New Mexico: New Mexico Bureau of Geology and Mineral Resources Open-File Geologic Map OF-GM 247, scale 1:24,000.

Koning, D.J., Aby, S.B., Jochems, A., Chamberlin, R., Lueth, V., and Peters, L., 2015, Relating ca. 5 Ma coarse sedimentation in the Rio Grande rift to tectonics, climate, and inter-basin fluvial spillover of the ancestral Rio Grande, in Proceedings, 2015 Annual Spring Meeting, Socorro, New Mexico: New Mexico Geological Society, p. 28.

Koning D.J., and Aby, S.B., 2005, Proposed members of the Chamita Formation, north-central New Mexico: in Lucas, S.G., Zeigler, K.E., Lueth, V.W., and Owen, D.E., eds., Geology of the Chama Basin: New Mexico Geological Society, 56th Annual Field Conference, Guidebook, p. 56, p. 258-278.

Lambert, P. W., 1966, Notes on the late Cenozoic geology of the Taos–Questa area, New Mexico: in Northrop, S.A., and Read, C.B., eds., Taos-Raton-Spanish Peaks Country (New Mexico and Colorado): New Mexico Geological Society, 17th Annual Field Conference, Guidebook, p. 43–50.

Le Bas, M.J., Le Maitre, R.W., Streckeisen, A., and Zanettin, B., 1986, A chemical classification of volcanic rocks based on the total alkali-silica diagram: Journal of Petrology, v. 27, p. 745-750.

Leininger, R. L., 1982, Cenozoic evolution of the southernmost Taos plateau, New Mexico [M.S. thesis]: Austin, University of Texas, 110 p.

Lipman, P.W., and Mehnert, H.H., 1979, The Taos plateau volcanic field, northern Rio Grande rift, New Mexico: in Riecker, R.C., ed., Rio Grande Rift: Tectonics and Magmatism: Washington, D.C., American Geophysical Union, p. 289–311.

Lipman, P.W., and Reed, J.C., Jr., 1989, Geologic map of the Latir volcanic field and adjacent areas, northern New Mexico: U.S. Geological Survey Miscellaneous Investigations Series Map I-1907, Scale 1:48000.

McKinley, P.K., 1957, Geology of the Questa quadrangle, Taos County, New Mexico: New Mexico Bureau of Mines and Mineral Resources Bulletin 53, scale 1:48,000, 23 p.

McMillan, N.J., and Dungan, M.A., 1986, Magma mixing as a petrogenetic process in the development of the Taos Plateau volcanic field, northern New Mexico: Journal of Geophysical Research, B, Solid Earth and Planets, v. 91, no. 6, p. 6029-6045.

McIntosh et al., 2004

Miller, J.P., Montgomery, A., and Sutherland, P.K., 1963, Geology of part of the southern Sangre de Cristo Mountains, New Mexico: New Mexico Bureau of Geology and Mineral Resources Memoir 11, 106 p.

Pazzaglia, F.J., 1989, Tectonic and climatic influences on the evolution of Quaternary landforms along a segmented range-front fault, Sangre de Cristo Mountains, north-central New Mexico [M.S. thesis], Albuquerque, University New Mexico, 246 p.

Peterson, C.M., 1981, Late Cenozoic stratigraphy and structure of the Taos Plateau, northern New Mexico: [M.S. thesis], Austin, University of Texas, 57 p.

Rehder, T.R., 1986, Stratigraphy, sedimentology, and petrography of the Picuris Formation in Ranchos de Taos and Tres Ritos quadrangles, north-central New Mexico [M.S. thesis]: Dallas, Southern Methodist University, 110 p.

Ruleman, C., Shroba, R., and Thompson, R., 2007, Chapter C – Field trip day 3; Quaternary Geology of Sunshine Valley and Associated Neotectonics along the Latir Peaks Section of the Sangre de Cristo fault zone: in Machette, M.N., Coates, M.M., and Johnson, J.L., eds., 2007 Rocky Mountain Section Friends of the Pleistocene Field Trip—Quaternary Geology of the San Luis Basin of Colorado and New Mexico, September 7-9, 2007, 24 p.

Shroba, R.R., and Thompson, R.A., 1998, Eolian origin of sandy mantles on gently-sloping basaltic lava flows in the Pliocene Cerros del Rio volcanic field near Santa Fe, New Mexico—Preliminary findings, in Slate, J.L., ed., U.S. Geological Survey Middle Rio Grande Basin Study—Proceedings of the second annual workshop, Albuquerque, New Mexico, February 10–11, 1998: U.S. Geological Survey Open-File Report 98–337, p. 24–25.

Thompson, R.A., Dungan, M.A., and Lipman, P.W., 1986, Multiple differentiation processes in early-rift calc-alkaline volcanics, northern Rio Grande rift, New Mexico: Journal of Geophysical Research, v. 91, p. 6046-6058.

Thompson, R.A., and Machette, M.N., 1989, Geologic map of the San Luis Hills area, Conejos and Costilla counties, Colorado: U.S. Geological Survey Miscellaneous Investigations Series Map I-1906, scale 1:50,000.

Thompson, R.A., and Schilling, S.P., 1988, Generalized geologic maps of the Brushy Mountain and Timber Mountain areas, Taos County, New Mexico: U.S. Geological Survey Open-File Report 88-561, 1 plate.

Thompson, R.A., Turner, K.J., Shroba, R.R., Cosca, M.A., Ruleman, C.A., Lee, J.P., and Brandt, T.R., 2014, Geologic Map of the Sunshine quadrangle, Taos County, New Mexico; U.S. Geological Survey Scientific Investigations Map 3283, scale 1:24,000.

Upson, J.E., 1941, The Vallejo formation; new early Tertiary red-beds in southern Colorado: American Journal of Science, v. 239, no. 8, p. 577-589.

Zimmerer, M.J., and McIntosh, W.C., 2012, The geochronology of volcanic and plutonic rocks at the Questa caldera: Constraints on the origin of caldera-related silicic magmas: Geological Society of America Bulletin, v. 124, no. 7/8, p. 1394-1408.